https://doi.org/10.5194/egusphere-2024-1463
Preprint. Discussion started: 4 June 2024

Downscaling the probability of heavy rainfall over the Nordic countries

Rasmus E. Benestad[1], Kajsa M. Parding[1], and Andreas Dobler[1]
[1]The Norwegian Meteorological Institute, Henrik Mohns plass 1, Oslo 0313, Norway
Correspondence: R.E. Benestad (rasmus.benestad@met.no)

Abstract. We used empirical-statistical downscaling to derive local statistics for 24-hr and sub-daily precipitation over the Nordic countries, based on large-scale information provided by global climate models. The local statistics included probabilities for heavy precipitation and intensity-duration-frequency curves for sub-daily rainfall. The downscaling was based on estimating key parameters defining the shape of mathematical curves describing probabilities and return-values, namely the annual wet-day frequency f_w and the wet-day mean precipitation μ. Both parameters were used as predictands representing local precipitation statistics as well as predictors representing large-scale conditions. We used multi-model ensembles of global climate model (CMIP6) simulations, calibrated on the ERA5 reanalysis, to derive local projections for future outlooks. Our analysis included an evaluation of how well the global climate models reproduced the predictors, in addition to assessing the quality of downscaled precipitation statistics. The evaluation suggested that present global climate models capture essential covariance, and there was a good match between annual wet-day frequency and wet-day mean precipitation derived from ERA5 and local rain gauges in the Nordic region. Furthermore, the ensemble downscaled results for f_w and μ were approximately normally distributed which may justify using the ensemble mean and standard deviation to describe the ensemble spread. Hence, our efforts provide a demonstration for how empirical-statistical downscaling can be used to provide practical information on heavy rainfall which subsequently may be used for impact studies. Future projections for the Nordic region indicated little increase in precipitation due to more wet days, but most of the contribution comes from increased mean intensity. The west coast of Norway had the highest probabilities of receiving more than 30 mm/day precipitation, but the strongest relative trend in this probability was projected over northern Finland. Furthermore, the highest estimates for trends in 10-year and 25-year return-values were projected over western Norway where they were high from the outset. Our results also suggested that future precipitation intensity is sensitive to future emissions whereas the wet-day frequency is less sensitive.

1 Introduction

Increasing atmospheric concentrations of greenhouse gases, such as carbon dioxide CO_2 and methane CH_4 from human activity, strengthen the greenhouse effect and bring on global warming as well as changes in the global hydrological cycle (IPCC, 2021). Such climate change can be simplified in terms of a sum of changes in local temperature and rainfall statistics, which may affect both nature and society. Global climate models (GCMs) and earth system models (ESMs[1]) are our primary

[1]Henceforth, we use the term 'GCM' when referring to both GCMs and ESMs.

https://doi.org/10.5194/egusphere-2024-1463
Preprint. Discussion started: 4 June 2024

tools for making projections of the future climate and represent main features of Earth's climate system, but they are not designed to describe the small scales and local climate change (Takayabu et al., 2015). Nevertheless, the local response to global warming can be estimated through downscaling, and international efforts on downscaling have been coordinated under the World Climate Research Programme (WCRP) coordinated downscaling experiment (CORDEX) (Gutowski Jr. et al., 2016). The term *downscaling* refers to the process of using large-scale information that GCMs are able to reproduce skillfully, on scales larger than their *minimum skillful scale* (Takayabu et al., 2015), and subsequently add additional information about inter-scale dependencies and systematic effects from fixed geographical factors. Hence, downscaling is distinct to bias adjustment which merely involves an adjustment of model output so that they have similar statistical characteristics as observations without further considerations of the GCMs' minimum skillful scale[2]. Results from GCMs are often downscaled to provide projections for a future climate on a regional or local scale, but the omnipresence of pronounced non-deterministic decadal variability (Deser et al., 2012) represents a challenge and a source of uncertainty (Hawkins and Sutton, 2009). The non-deterministic chaotic contribution from natural and internal regional variations complicates the assessment of the credibility and robustness of ensemble projections, and one question is how to synthesize them into user-relevant information. This is highly relevant for results from downscaling approaches on national climate service levels for instance within the European downscaling efforts in EURO-CORDEX.

Another source of uncertainty in downscaled climate projections is connected to methodological choices and assumptions (Jacob et al., 2020). There are two main approaches in downscaling: (i) dynamical downscaling with regional climate models (RCMs) and (ii) empirical-statistical downscaling (ESD). The former has often been more visible within CORDEX, many climate service providers as well as impacts and adaptation communities (Rampal et al., 2024), and CORDEX data often refers to a set of RCM simulations excluding ESD results, e.g. the IPCC interactive atlas[3]. The one-sided focus may be a legacy of the past European projects PRUDENCE (2001-2004) and STARDEX (2002–2005) which had their distinct focus (Christensen et al., 2007; Christensen and Christensen, 2007; Goodess et al., 2003), however, results from STARDEX didn't indicate that RCMs were superior in terms of reproducing information about extreme rainfall (Haylock et al., 2006). Traditionally, ESD has been used to estimate small-scale (local) temperature or precipitation in terms of daily variability or aggregated statistics over months, seasons or years (Maraun et al., 2015), and downscaling of heavy precipitation has mainly involved dynamical downscaling with RCMs, while the merits of ESD perhaps have not been so widely recognised.

One advantage with ESD is that it requires little computational resources which makes it suitable for downscaling large multi-model ensembles (Benestad, 2011; Mezghani et al., 2017). Furthermore, ESD can be designed so that it's transparent and easily traceable, as the R-markdown script in this paper's supporting material tries to facilitate (Benestad, 2024). It is also possible to estimate various statistical aspects on precipitation through ESD, and Trenberth et al. (2003) argued that the characteristics of precipitation are just as vital as the amount. The characteristics of rain may indeed be more apt to change as climate changes, and some key statistics on precipitation involve both the typical amount falling on a rainy day (wet-day

[2]There are, however, ESD methods that are closer to bias correction, downscaling grid points separately and hence not taking minimum skillful scale into consideration. For example, NASA's NEX-GDDP data set (https://www.nccs.nasa.gov/services/data-collections/land-based-products/nex-gddp) is presented as downscaled climate scenarios but the method is a type of bias correction.

[3]https://interactive-atlas.ipcc.ch/regional-information/about

https://doi.org/10.5194/egusphere-2024-1463
Preprint. Discussion started: 4 June 2024

mean precipitation μ), how often it rains (wet-day frequency f_w), how long it is between each rainfall (dry-spell duration or number of consecutive *dry* days n_{dd}), the duration of wet-spells (number of consecutive *wet* days n_{wd} to account for clustering of precipitation events in time), the spatial extent of the precipitation (Lussana et al., 2024), and its phase (rain/snow). Here we will show how ESD can be designed to extract information on precipitation statistics such as probabilities of exceeding a certain threshold and intensity-duration-frequency curves.

There have been many studies on mean trends or extreme precipitation, but less on moderate heavy rainfall. Extremes often involves either general extreme value theory (GEV) calibrated with block maxima or the General Pareto distribution with peak over threshold, thus fitting the tails of the distribution (Coles, 2001). GEV also involves fitting the three parameters *location*, *scale* and *shape* which are often not well constrained for limited samples of block maxima. Statistical models for moderate intense events, on the other hand, may be calibrated from the bulk of the data sample with fewer parameters (f_w and μ), and may be easier to evaluate when time series only span a few decades. Furthermore, if the parameters have a more straight-forward physical interpretation, they may also serve to enhance our understanding of shifts in the statistics. Moderate extremes, such as merely 'heavy rainfall' (e.g. 20–50 mm/day), may also trigger landslides, cause erosion, and affect the spread of water-borne disease or eco-toxins. Furthermore, since GCMs only provide a coarse large-scale representation of the real climate system, it is necessary to use downscaling methods that are not degraded too much by their lack of precision. Hence we aimed for a robust and approximate method for downscaling 24-hr precipitation statistics, to some extent scarifying its exactitude which perhaps could be obtained through a sophisticated representation in an ideal setting (e.g. GEV). Furthermore, multi-variable predictors (common in traditional downscaling and in machine learning) place great and unrealistic demands on GCMs because different variables simulated by a GCM may be strongly correlated with the predictand over a historical calibration period, but may evolve in different directions in the future (Parding et al., 2019). In other words, we expect a trade-off between exactitude and robustness, and hence we aimed for robust, reliable low precision, and approximate results for moderate extremes in our case.

2 Data and Methods

2.1 Data

The daily rain gauge data used in this analysis were collected from the ECA&D (Klein Tank et al., 2002) within the latitude range 55–71°N and longitude range 5–30°E. The initial selection comprised 2131 rain gauges as predictand covering the time interval 1950–2021 from Belarus (4), Denmark (14), Estonia (27), Finland (443), Germany (1), Latvia (29), Lithuania (13), Norway (669), Russian (11), and Sweden (920), located at a range of elevations, the highest point being 2062 above sea level. Only rain gauge records with sufficient number of valid data were included in the subsequent downscaling, and rain gauge measurements from only 652 locations remained in our predictand after short station records had been removed. Figure 1 shows the geographical distribution of the rain gauges and their mean annual total rainfall. The analysis was based on key aggregated statistics: annual wet-day frequency f_w and annual wet-day mean precipitation μ. We used the threshold of 1 mm/day to distinguish between dry and wet days. Annual f_w and μ with the same threshold were also used as predictors and were estimated from both the ERA5 reanalysis (Hersbach and Dee, 2016; Hersbach et al., 2020) as well as GCMs.

https://doi.org/10.5194/egusphere-2024-1463
Preprint. Discussion started: 4 June 2024

The GCM data was taken from CMIP6 (Eyring et al., 2015, 2016) for historical runs (HIST) as well as various emission scenarios (SSP370, SSP126, SSP245, and SSP585) described in IPCC (2021). Only a subset of GCM runs were included here as daily precipitation was needed to estimate annual f_w and μ for use as predictors. To reduce the data transfer amount, server-side data processing facilities at the German Climate Computing Centre (DKRZ) were used to derive the annual values with the climate data operators (CDO) software (Schulzweida, 2021) installed on site. Nevertheless, a great deal of effort was required to derive f_w and μ from ERA5 and all CMIP6 runs, and hence we make a case for a standard protocol for reanalysis and CMIP data archive that includes monthly f_w and μ. The predictors f_w and μ from CMIP6 HIST simulations were evaluated against ERA5 following Benestad et al. (2023), testing the GCMs' ability to reproduce the mean seasonal cycle, interannual variability in annual f_w and μ and their historical trends, and one simulation (CESM2-WACCM-FV2) was removed due to poor evaluation results. Our analysis focused on 29 model runs following SSP370, but the other emission scenarios are included in the supporting material (Benestad, 2024).

2.2 Downscaling methodology

Our analysis introduces a new aspect in terms of downscaling by using large-scale wet-day mean precipitation μ as predictors for estimating station-level μ, the predictands, as well as using large-scale wet-day frequency f_w as predictors to downscale local f_w at a station level. Both these types of predictors were estimated from the ERA5 reanalysis and CMIP6 GCMs for the region in question, using common empirical orthogonal functions (henceforth 'common EOFs') as a framework for representing both the real world and modelled conditions (Benestad, 2001). This choice implied using a so-called '*hybrid PP-MOS*'[4] framework to represent the predictors and ensured that those from ERA5 used for calibration matched those from GCMs used for projection. The introduction of the ERA5 reanalysis has been a step change in terms of progress within ESD, as there was a close match between f_w and μ from the reanalysis and rain gauge measurements respectively (see the supporting material), enabling their use as predictors. Details about the ESD set-up and analysis are accounted for in the R-markdown script provided as supporting material, together with all the results generated.

Principal component analysis (PCA) (Wilks, 2006) was used to represent the predictands as it tends to emphasise large-scale structures in groups of local measurements (Benestad and Mezghani, 2015), and a step-wise multiple ordinary linear regression (OLR) was used to find an optimal connection between principal components representing the large-scale predictors and the principal components representing local f_w and μ. In this case, 5 leading PCA modes were used to represent the most salient information of annual f_w and μ estimated from the rain gauge measurements, representing 100% of the variance in the station-based statistics for both. We used the 7 leading EOFs (Lorenz, 1956) estimated for f_w or μ from ERA5 in a step-wise multiple regression to estimate each PCA mode for the corresponding predictand. The PCA was implemented though the means of a singular value decomposition (SVD) where U represented the spatial weights ('geographical pattern'), Λ held the eigenvalues (variances), and V contained the time series (principal components, PCs, used in the regression analysis) according to

[4]https://cordex.org/wp-content/uploads/2022/08/White-Paper-ESD.pdf

https://doi.org/10.5194/egusphere-2024-1463
Preprint. Discussion started: 4 June 2024

$$x = U\Lambda V^T. \quad (1)$$

Time series representing f_w and μ were generated from downscaled estimates of V and subsequently computed according to equation 1. The downscaled annual f_w and μ were subsequently used to estimate the probability that daily precipitation amount (X) exceeded a given threshold (x) using the simple and approximate relation $Pr(X > x) \approx f_w \exp(-x/\mu)$ based on Benestad et al. (2019). The analysis for daily precipitation amounts was extended to sub-daily timescales where the shape of intensity-duration-frequency (IDF) curves was downscaled based on their dependency on $x_\tau = \alpha\mu(L/24)^\zeta \ln(f_w\tau)$, where α was a calibrated adjustment factor, L was the duration of wet-spells in hours, and ζ described the fractal dimension for temporal scale inter-dependencies (Benestad et al., 2020). The results for the sites of the rain gauge measurements were subsequently gridded through kriging of the spatial weights (U in equation 1) with elevation as a co-variable using the R-package `LatticeKrig` (Nychka, 2014), and the downscaling itself was carried out using `esd` (Benestad et al., 2015).

2.3 Evaluation

The evaluation of the models and methods are documented in the supporting material (Benestad, 2024) and was applied to downscaled results through cross-validation and testing whether the observations belonged to the same statistical population as the downscaled multi-model ensemble. There was a close match between the aggregated rain gauge data and ERA5 for both f_w and μ, where the cross-validation was 0.93 for the leading PCA mode for annual f_w, accounting for 50% of the variance. The downscaling exercise for the second PCA (29% of the variance) gave a cross-validation correlation of 0.92. Furthermore, the geographical weights of the calibrated ERA5 predictor matched spatial patterns of corresponding PCA mode, as should be expected when the same variable is used as both predictor and predictand. Similarly, the downscaling exercise between aggregated rain gauge and ERA5 for annual μ returned cross-validation correlations of 0.96 and 0.81 for first and second PCA modes respectively (representing 54 and 26% of the variance respectively), with matching spatial weights between calibrated ERA5 data and PCA modes. Moreover, similar geographical distribution of spatial weights in the predictors and predictands indicates a good match between the ERA5 and rain gauge measurement annual precipitation statistics when both involve the same variable.

The evaluation also involved testing the ability of the GCMs in reproducing the predictors in a skillful way. The test of simulated predictor quality used common EOFs (Barnett, 1999) to compare the spatio-temporal covariance structure captured by simulations with corresponding information derived from ERA5 reanalysis, as in Benestad et al. (2023) but applied to f_w and μ respectively (supporting material). The CMIP6 GCMs reproduced the mean seasonal cycle in f_w and μ aggregated from the ERA5 reanalysis, as well as the historical interannual mean variability in the annual f_w and μ (for the period 1959–2021). A comparison of historical trends in GCM historical runs and ERA5 further indicated that the GCMs were able to reproduce the observed historical changes in f_w and μ. The CMIP6 ensembles for f_w and μ were of limited size since they were generated from daily data and e.g. monthly f_w and μ values are not (yet) part of the CMIP standard output protocol. We thus limited our analysis to one particular configuration from each GCM (e.g. r1i1p1f1). The number of ensemble members of regional

https://doi.org/10.5194/egusphere-2024-1463
Preprint. Discussion started: 4 June 2024

or local climate projections can be interpreted as equivalent to statistical sample size, as each model simulation involves non-deterministic stochastic decadal variability (Deser et al., 2012). The normal distribution may provide useful information on statistical data samples with about 30 data points if the data are normally distributed, and hence, distributions of downscaled ensemble results were tested against a normal distribution as in Benestad et al. (2023). The results of these tests suggested that the ensemble mean and standard deviation can provide an approximate description of the ensemble.

The evaluation of both downscaling method and the GCM simulations established that local wet-day frequency f_w and wet-day mean precipitation μ can be skillfully estimated over the Nordic region from corresponding large-scale quantities from both the ERA5 reanalysis and CMIP6 simulations. The subsequent step was to use these results to make projections for future climatic outlooks and estimate changes in precipitation statistics, based on relationships established from previous studies (Benestad et al., 2019, 2020). Such steps are to the best of our knowledge the first efforts to downscale statistical properties for daily precipitation directly beyond downscaling extreme climate indices (Goodess et al., 2003; Haylock et al., 2006).

3 Results

Figure 2 shows time series for the wet-day frequency f_w and wet-day mean precipitation μ extracted for Oslo-Blindern, and the black symbols show the annual statistics derived from historical measurements, whereas the green band shows corresponding statistics downscaled from the CMIP6 SSP370 multi-model ensemble. Neither the observations nor the projections indicated any pronounced trend in the annual f_w for Oslo, however, statistics based on rain gauge measurements over all the Nordic sites nevertheless suggested a general weak increase in the number of wet days over the 1950–2021 period that was statistically significant at the 5%-level (supporting material). The downscaled projections for Oslo (green shading in Figure 2 and the Nordics (lower left panel in Figure 3), however, indicated a weak (geographically mixed and non-significant) general decrease in number of wet days for the period 2015–2099, based on the ensemble mean of the CMIP6 simulations following the SSP370 emission scenario. Other emission scenarios gave some variations in the outlook, and the SSP126 as well as the SSP585 results gave a more mixed picture of trends in future f_w, (supporting material). The trend estimates in f_w were expected to vary with the frequency of weather types, and the forces driving the atmospheric circulation that characterise different weather types tend to arise from variations in the distribution of atmospheric mass which is not necessarily strongly constrained by an increased greenhouse effect. However, there has been as slight trend in annual f_w in Oslo that was reproduced in a downscaling exercise using ERA5 as predictor (supporting material).

There has also been a modest increase in annual wet-day mean precipitation μ that was more pronounced than the trends in f_w, which also is visible in Figure 2 (right panel) and Figure 3 (lower right panel). The trend estimates in μ were more spatially consistent within the various emission scenarios, although higher emissions were connected to stronger trends, and the results indicated increases for most of the region except in the vicinity of Troms municipality in northern Norway. Table 1 presents the ensemble mean and standard deviation for a small selection of locations projected for the period 2071–2100. The downscaled results suggested that projected trends in f_w were not sensitive to the emission scenario (SSPs), however, the magnitude of projected trends in μ ranked in increasing magnitude for SSP126, SSP245, SSP370, and SSP585 respectively.

https://doi.org/10.5194/egusphere-2024-1463
Preprint. Discussion started: 4 June 2024

Since the mean precipitation is the product of the wet-day frequency and wet-day mean precipitation[5] we estimated trends in total precipitation and can explain total precipitation changes in terms of changing number of wet days or changing intensity. Figure 4 shows estimated future trends in precipitation (mm/day per decade in upper panel: $dx/dt = \mu df_w/dt + f_w d\mu/dt$) as well as its contribution from changing number of wet days (lower left) and changes in mean precipitation intensity (lower right). The projections of the future climate in the Nordic region indicated a general increase in the total precipitation mainly due to increased wet-day mean precipitation μ and in spite of decreased wet-day frequency f_w, according to the selected CMIP6 simulations.

The wet-day frequency f_w and wet-day mean precipitation μ represent two key parameters for approximate estimation of the probability of heavy rainfall according to $Pr(X > x) = f_w \exp(-x/\mu)$ (Benestad et al., 2019). Figure 5 shows observed fraction of days per year with more than 30 mm for Oslo-Blindern (black symbols) compared with such low-precision estimates based on the ensemble mean (red solid line) shown with error bars of one standard deviation (red dashed). The statistics based on rain gauge measurements and information downscaled from the GCM ensembles indicated somewhat matching levels, however, the observations included some years with substantially higher numbers of days with heavy rainfall. These results nevertheless serve as an example where probabilities for heavy rainfall have been downscaled directly though the parameters f_w and μ, as opposed to aggregating data points from of a statistical sample containing traditionally downscaled time sequences of weather states. Another benefit with a parameterised expression for probability was that we could differentiate it according to the product rule: $dPr(X > x)/dt = (df_w/dt)\exp(-x/\mu) + f_w x/\mu^2 \exp(-x/\mu)(d\mu/dt)$. Figure 6 shows maps of both $Pr(X > x)$ and percentage trends ($100 \times dPr(X > x)/Pr(X > x)$) for the SSP370 ensemble mean, and the results indicated highest probabilities for days receiving more than 30 mm of precipitation on the west coast of Norway, but the relative trends were greatest over northern Finland.

The parameterised expression for probabilities also enabled downscaling of return-values $x_\tau = \alpha\mu \ln(f_w\tau)$ where α is a calibration coefficient (Benestad et al., 2019). Figure 7 shows both 10-year (left panels) and 25-year (right panels) return-values as well as their estimated trends (lower panels) based on the ensemble mean SSP370 results. The greatest return-values were estimated over western Norway, with 10-year estimates ranging in 30–170 mm/day while 25-year estimates varied within the range 40–220 mm/day. The lowest estimates were downscaled for parts of northern Finland, Sweden and Norway. Projected future trends in x_τ were estimated based on trends in the wet-day frequency df_w/dt and wet-day mean precipitation $d\mu/dt$ (lower panels in Figure 3), the above expression and the product rule, and increases in x_τ were in general a result of increasing mean intensity rather than more wet days. The greatest trends in the return-values dx_τ/dt were downscaled over western Norway with already high levels, but there were also notable increases over southwestern Finland and over parts of southwestern Sweden.

Downscaled f_w and μ also provided first-guess estimates for intensity-duration-frequency (IDF) curves, assuming there was a fractional dependence between temporal scales. We based our estimates of IDFs on Benestad et al. (2020), using the expression $x_\tau(L) = \alpha\mu(L/24)^\zeta \ln(f_w\tau)$ which describes mathematical curves whose shapes are approximately similar to IDF curves estimated through more traditional means, where L is the duration in hours and ζ describes the fractional dependency

[5] $\overline{x} = \sum x/n_w \times n_w/n = f_w\mu$ where $f_w = n_w/n$ and $\mu = \sum x/n_w$.

https://doi.org/10.5194/egusphere-2024-1463
Preprint. Discussion started: 4 June 2024

between temporal scales and was fitted to observational rain gauge measurement data. We estimated how the shape of IDF curves may change due to trends in f_w and μ (their trends are shown in the lower panels in Figure 3), and IDFs for Oslo for present and the future are shown in Figure 8. Different estimates for IDFs for the present $x_\tau(L)$ and the future $x'_\tau(L)$ provide an opportunity to estimate scaling factors for IDF curves $x'_\tau(L)/x_\tau(L)$ to account for further climate change: 1.13–1.14 for f_w and μ projected with SSP370 ensemble mean, not taking into account decadal variability. A crude measure for accounting for decadal variability was to use the ensemble spread $\pm\sigma$, and subtracting σ for the present and adding σ in the future gave scaling factors within the range 1.18–1.20 for SSP370. For higher emissions associated with SSP585, the scaling factors were 1.27–1.38, in this case only based on the ensemble mean and not accounting for decadal variability. All these estimates varied with the return-period τ, but the scaling factors were the same across time durations L in accordance with the expression above. In this case, we assumed that α and ζ were constant for a given site.

We also explored the connection between the wet-day frequency and duration of dry spells (number of consecutive dry days), which may provide some indication of meteorological drought risk (supporting material). The calibration of our ESD method indicated that there was a link between large-scale f_w from ERA5 and the mean duration of dry spells. The spell duration approximately followed a geometric distribution where the mean duration (number of consecutive dry days) was the inverse of the "success" probability, which implies that we approximately could estimate the probability of a dry spell lasting longer than a given threshold. A projected weak reduction in f_w over the Nordic region will therefore suggest slightly increased risks of meteorological droughts in the future.

4 Discussions

To our knowledge, this is the first time the shape of curves representing probabilities for heavy rainfall or IDF curves have been downscaled using a hybrid PP-MOS approach (which addresses the '*domain adaption*' aspect discussed in Rampal et al. (2024)) applied to multi-model GCM ensembles, albeit estimating the parameters defining their shapes. Those parametric expressions nevertheless enabled us to analyse the causes for trends in precipitation, probabilities, return-values, probability of meteorological droughts, or for shifts in the shape of IDF curves. These statistics were calculated from formulas which used downscaled f_w and μ as input, and the results underscored that both the wet-day frequency and the wet-day mean precipitation are two key parameters for describing precipitation. In our case, the results were more sensitive to the mean precipitation intensity μ than wet-day frequency f_w.

Our results suggested a slight reduction in the future wet-day frequency over the Nordic countries which may reflect predominant changes in the atmospheric circulation patterns, due to the location of storm tracks and blocking high-pressure systems. Present state-of-the-art GCMs still have biases when it comes to storm tracks and blocking frequencies, which is possibly due to a coarse representation of the polar jet stream and other processes in the Arctic (IPCC, 2021). The downscaling may underestimate long-term changes in the mean precipitation intensity μ, even if the evaluation of the CMIP6 models seemed to score well on the comparison between trends in GCMs and ERA5. A separate test where μ was downscaled solely based on ERA5 reanalysis didn't capture the historical changes observed in Oslo (supporting material). Furthermore, the projections of

https://doi.org/10.5194/egusphere-2024-1463
Preprint. Discussion started: 4 June 2024

wet-day frequencies f_w didn't account for the risk that circulation patterns may change in ways not captured by present models. There may also be tipping points in the North Atlantic and sea ice cover, changes in the jet stream, effects from displaced storm tracks, and inaccurate blocking high frequency (IPCC, 2021) uncovered by the model projections. Nevertheless, a take-home message is that long-term trends in μ were sensitive to future emissions.

This analysis has explored annually aggregated f_w and μ, but the presence various meteorological phenomena tend to vary with the seasons and a mean annual trend may mask possible opposite trends in different regions. To assess this possibility we took a random sample from historical rain gauge measurements from Oslo and compared seasonal trends in both f_w and μ (supporting material). Our random test suggested that there were no pronounced opposite trends, but a more thorough exercise would entail downscaling seasonal mean precipitation statistics for the Nordic region. We leave the task of seasonal focus for the future, as a part of our objectives was to develop and evaluate downscaling approach for the EU-SPRINGS project and to provide the first projections for the planned national report 'Klima i Norge, 2100'. This strategy will also be explored in collaboration with Mozambique through CORDEX flagship pilot study (FPS) southeast Africa and the Norad-funded project SAREPTA[6]. This 'downscaling climate' approach for precipitation may work even if there is limited rain gauge data but it is important that reanalyses such as ERA5 correspond well with data on the ground.

Our results show the merit of the 'downscaling climate' approach which is not as wide-spread as downscaling of time sequences with individual atmospheric states. However, all expressions used here in connection with ESD can also be combined with RCMs, as Oguz et al. (2024) used the EURO-CORDEX ensemble (RCMs) rather than ESD to estimate f_w and μ. They subsequently used the IDF curves as a basis for weather generators (Monte-Carlo simulations) to provide input for landslide modelling. Nevertheless, based on their utility, the wet-day frequency f_w and the wet-day mean precipitation μ should be listed among essential climate indicators[7], and they should be included in the standard output from reanalysis, GCMs (e.g. CMIP[8]) and RCMs (CORDEX[9]), e.g. as monthly mean f_w and μ. The CMIP ensemble here was limited to one simulation per GCM because f_w and μ had to be estimated from available daily output, making it difficult to explore uncertainties connected to initial conditions, natural variability as well as model choices (Mezghani et al., 2019). However, it may be possible to use factorial regression or ANOVA to assess how model choice affects the downscaled ensemble with larger multi-model ensembles that include multiple simulations with the same GCM (Benestad et al., 2017, 2016). With the available CMIP6 data in this case, it was only possible to carry out an assessment of the sensitivity to emissions through comparing downscaled results from SSP126, SSP245, SSP370 and SSP585.

It's important to combine equivalent results from both ESD and RCMs when downscaling is used to produce regional or local climate projections for the future, since they are based on different assumptions and have different strengths and weaknesses but are expected to give similar results for aggregated precipitation and temperature. Such an intercomparison is done for surface air temperature and precipitation in Parding et al. (in progress), but the purpose of this study was to examine the potential for downscaling daily various precipitation statistics with ESD. We leave a comparison with similar information from RCMs for

[6]https://bistand.met.no/en/Sarepta
[7]https://gcos.wmo.int/en/essential-climate-variables/
[8]https://esgf-data.dkrz.de/search/cmip6-dkrz/ or https://cds.climate.copernicus.eu/
[9]e.g. https://esgf-data.dkrz.de/search/cordex-dkrz/

https://doi.org/10.5194/egusphere-2024-1463
Preprint. Discussion started: 4 June 2024

future work, and it is also important to account for chaotic and stochastic variability on regional and decadal scales (Deser et al., 2012), for instance using large multi-model ensembles as a surrogate for statistical sampling and letting the ensemble spread give a crude representation of probable outcomes. This analysis suggested that the ensemble spread for both annual f_w and μ were approximately normal which implies that the ensemble mean as well as standard deviation may provide useful information about the ensemble spread.

While RCMs and traditional ESD provide output for a sequence of atmospheric states on daily or sub-daily resolution, which we can refer to as weather conditions, our strategy has been to downscale parameters for local probability, rather than estimating the statistics from samples made up of such data sequences. We can loosely refer to the former as '*downscaling weather*' whereas the latter can be termed '*downscaling climate*' if climate can be defined as weather statistics or probability density functions (pdfs) reflecting (sub-)daily precipitation amounts. Statistical properties of precipitation are expected to follow a more systematic geographical distribution than any random individual weather event, being influenced by prevailing large-scale conditions as well as fixed local geographical factors. Our objective was to downscale parameters describing the shape of a pdf or similar mathematical curves, and this approach was first inspired by Pryor et al. (2005, 2006) and is based on a long-term effort and a series of projects (e.g. EU-SPECS, KlimaDigital). The 'downscaling climate' approach can also be applied to e.g. summertime heatwaves or used to downscale the probability of the occurrences n_H as well as duration of hot spells $\overline{L_H}$ (Benestad et al., 2018), however, heatwaves were beyond the scope of the present analysis. Another example of the merit of this concept is the downscaling of storm track density (Parding et al., 2019), and future work in the EU-SPRINGS project will explore the possibility to downscale public health statistics for water-borne diseases that may lead to diarrhoea.

One question is whether the fractal temporal scaling properties utilised in the approximate IDF representation in Figure 8 is stable or if we can expect it to change in time and space. Dobler et al. (in progress) has examined aspects of these scaling properties based on convective-permitting RCMs over the Nordic countries and found weak geographical variations consistent within an RCM driven by different boundary conditions, but we must expect them to change if some meteorological phenomena with certain typical time scales become more prominent than others in the future (e.g. convective compared to frontal precipitation).

Our results suggested that the annual wet-day frequency f_w was more coherent over space, as all the 20 leading EOFs combined accounted for 88% of the variance in the ERA5 reanalysis compared to 74% for the annual wet-day mean precipitation μ. Moreover, the leading EOF mode for the annual wet-day mean precipitation μ from ERA5 captured 19% of the variance as opposed to 30% for f_w, which suggests that μ to a greater degree reflects small scale processes and phenomena not being as strongly correlated over the region on annual time scales. Local and mesoscale processes and phenomena that may influence μ include surface-air fluxes, and local geographical effects such as orographic forcing. However, both f_w and μ are expected to reflect meteorological phenomena ranging from local microscale, mesoscale and synoptic scales that may produce precipitation with different characteristics, dynamics and mechanisms, including convection, cut-off lows, mid-latitude cyclones, frontal systems, atmospheric rivers, and orographic forcing. Both increased precipitation amount from higher surface temperature as well as changes in the distribution of the precipitation over the planetary surface play a role in the trends in extreme precipitation amounts. Benestad et al. (2024) found a link between increased intensity on the one hand and increased rate of evaporation

https://doi.org/10.5194/egusphere-2024-1463
Preprint. Discussion started: 4 June 2024

as well as changes in the global surface area receiving daily precipitation on the other. They also observed that changes in the global fractional surface area with daily precipitation were connected to the global statistics of the wet-day frequency f_w.

Using the same variables for predictors and predictands, as in his case, leaves it up to the GCMs to represent the underlying phenomena that generate precipitation. We could refer to this strategy as a hybrid 'SR-MOS' in the terms proposed by Rampal et al. (2024) rather than 'PP-MOS', however, we stick to 'PP-MOS' for simplicity. Improved GCMs in the future may reproduce various meteorological phenomena and processes with improved skill which may lead to better estimates for future projections. It is also important that the reanalysis used for calibration match the predictands closely.

Our results were produced with a hybrid PP-MOS strategy for downscaling climatic parameters represented through PCAs that may serve as a benchmark for machine learning and artificial intelligence (Rampal et al., 2024). In addition to combining ESD and RCMs because they are based on different assumption, there is value in combining this ESD approach with more advanced machine learning (ML) or artificial intelligence (AI) methods that produce results with very different constraints. However, since downscaling f_w and μ doesn't require as large data volume or as long time series as either ML/AI or traditional methods for studying extremes, such a comparison will be limited to cases with ample observational data or 'pseudo-realities' using model output. One merit of our strategy is that it provides an explainable method which enhances our understanding of projected changes and thus compliments many ML/AI methods. Hence, our downscaling strategy addresses some of the research questions stated in Rampal et al. (2024), and when the recipe of the entire analysis can be documented through an R-markdown script (supporting material), it's easier to provide transparency and traceability sought within scientific discourse.

5 Conclusions

We used the ERA5 reanalysis and local rain gauge measurements from the Nordic countries to calibrate empirical-statistical downscaling models which were applied to CMIP6 projections, using annual wet-day frequency f_w and wet-day mean precipitation μ respectively both as predictors and predictands. A good match between ERA5 reanalysis and rain gauge measurements for these two key statistics over the Nordic region gave a good calibration of our downscaling method. Predictors from global climate models from CMIP6 were evaluated and scored well in terms of their ability to represent mean seasonal variations, interannual variability of annual aggregates and past trends, and our downscaling used a hybrid PP-MOS approach for estimating parameters for mathematical curves providing actionable regional climate information. The downscaled f_w and μ were subsequently used to estimate local probabilities for heavy rainfall, return values and changes in the shape of intensity-duration-frequency curves. We used kriging with elevation as covariate to generate Nordic maps of f_w and μ and their projected changes. Projected changes in the future suggest increases in μ but very slight decreases in f_w, hinting at less frequent or similar level of wet days in the future but also more intense rainfall. The amplitude of projected trend in μ was sensitive to the emission scenario, but trends in f_w were not. The spread between the ensemble members was approximately normally distributed, which implies that essential information about the ensemble may be captured through the ensemble mean and standard deviation.

https://doi.org/10.5194/egusphere-2024-1463
Preprint. Discussion started: 4 June 2024

Code availability. The R-markdown script, on which this analysis is based, is provided in the supporting material and available from FigShare (Benestad, 2024)

Appendix A: Summary of the supporting material: R-markdown output

- EOF on annual f_w from ERA5: 20 combined EOFs 88%. Leading EOF 30%, 2nd EOF 19%.
- PCA annual f_w from ECA&D: 20 combined EOFs 100%. Leading PCA 50%, 2nd PCA 29%.
- Downscaling exercise on ERA5 reanalysis gave cross-validation correlations for the two leading PCAs of 0.93 and 0.92 respectively. The results gave similar spatial weights in predictors and predictands, also suggesting a good match.
- EOF annual μ ERA5: 20 EOFs 74%. Leading EOF 19%, 2nd EOF 9%.
- PCA annual μ ECA&D: 20 EOFs 100%. Leading PCA 54%, 2nd PCA 26%.
- Downscaling exercise on ERA5 gave cross-validation correlations for the two leading PCA modes of 0.96 and 0.81 respectively and similar spatial weights in predictands and predictors, suggesting strong calibration.
- Historical trends: general increase in f_w from ECA&D, mainly during winter.
- General increase in μ from ECA&D, mainly during winter, most pronounced in spring.
- Oslo: the observed number of days with more than 20 mm/day precipitation correlates with estimated probability. Estimated probability for more than 10 mm/day from ensemble mean and standard deviation wide error bars and a slight high bias. Less bias for 20 mm/day and 30 mm/day.
- Downscaled annual f_w and μ projected changes were used to estimate IDF for present and future, as well as estimating scaling factors meant to capture the effect of climate change.
- The mean duration of dry spells (number of consecutive dry days) in Oslo correlated with large-scale f_w over the surrounding region (ERA5).
- Exercise to downscale number of days per year with more than 20 mm/day directly from ERA5 predictors failed to capture spikes and peaks. Only modest cross-validation correlations.
- Downscaled f_w indicated highest values along the coast for all emission scenarios, and future trends indicated a slight reduction in the number of wet days over most of the region in SSP370 - in a slight contrast with historical observations. The projected trends in f_w were more mixed for SSP126, but mainly dry in SSP245. There was a sharper contrast between the west coast (more wet days) and the interior parts (less wet days) of the Nordic countries for downscaled f_w from SSP585.

https://doi.org/10.5194/egusphere-2024-1463
Preprint. Discussion started: 4 June 2024

- Downscaled μ indicated highest values along the coast for all emission scenarios, and future trends indicated an increase in the mean precipitation intensity over most of the region in SSP370. The projected trends in μ were weaker for SSP245. There was a sharper contrast between the region around Troms (reduced intensity) and the rest of the Nordic countries for downscaled μ, and this was more pronounced in SSP585. SSP126 was not plotted due to some data format problems.

- The trend in mean precipitation estimated from both f_w and μ indicated general increases except for three spots: part of southeastern Norway, parts of interior southern Sweden and the region around Troms. Most of the trend was due to increases in the mean precipitation intensity, as the contribution from reduced number of wet days in general pulled the trends towards drier conditions.

- The probability of more than 30 mm/day was highest on the west coast of Norway (up to 0.1), and estimated absolute trends were also greatest in the same region. But the relative trends (trend/mean) were highest over southern Finland. The trend in probability was mainly due to increased mean precipitation intensity, but the number of wet days also contributed over parts of Norway (Møre og Romsdal, Trøndelag and southern parts of Nordland) and southern Finland and Estonia.

- 1-year, 10-year and 25-year return values were estimated to have highest values along the western coast of Norway. The estimated tends in these return-values were also highest in the region where they were high from the outset.

- The evaluation of CMIP6 f_w against ERA5 on par with Benestad et al. (2023) suggested that the GCMs reproduced the mean annual cycle, interannual variability in annual f_w and trend in f_w over the Nordic region. The leading EOF for the annual cycle accounted for 70% of the variance, the second mode 16% and the combined 20 leading modes 99%, suggesting that the GCMs simulated similar spatial patterns and seasonal variations. The leading EOF for interannual variations in annual f_w was 37%, the 2nd 16%, and the 20 leading modes 90%, suggesting a slightly greater degree heterogeneity than for the mean seasonal cycle, but still generally similar variability. For the assessment of trend maps from each GCM and ERA5, the leading EOF explained 45%, 2nd mode 16 and the leading 20 EOFs 99%, suggesting that also the spatial trend maps bore similarities. The covariance structure at the core of the ESD method and this evaluation was designed to examine the model skill in reproducing it.

- One CMIP6 member (CESM2-WACCM-FV2) differed from the rest of the ensemble and was omitted from the downscaling to provide future projections. This also applied to μ.

- The evaluation of CMIP6 μ against ERA5 suggested that the GCMs reproduced the mean annual cycle, interannual variability in annual μ and trend in μ over the Nordic region. For the mean seasonal cycle, the leading EOF accounted for 69% of the variance, 2nd 20% and the combined 20 leading modes 98%. For interannual variability in annual μ, the first, second and combined 20 leading EOFs explained 21%, 13% and 75% respectively. The EOF analysis applied to trend maps for each member plus ERA5 gave 70%, 6% and 99%. All GCMs reproduced the strongest variability in μ near the west coast of Norway.

https://doi.org/10.5194/egusphere-2024-1463
Preprint. Discussion started: 4 June 2024

Author contributions. REB conceptualised, carried out most of the analysis, and drafted the paper; AD processed CMIP data and contributed to writing up the paper; KP has contributed to method development within the R-package `esd` and writing.

Competing interests. None

Disclaimer. The future projections are only as good as the GCMs on which they are based. They are the best information we have at the time of this analysis, are based on various assumptions, and there is always a risk that unaccounted for factors also play a role and may result in a different future climatic evolution.

Acknowledgements. This work aimed to benefit the following projects and networks: EU-SPRINGS (Project number 101137255 - HORIZON-HLTH-2023-ENVHLTH-02), Klima i Norge 2100 (Met Norway), SAREPTA (Norad), and CORDEX-ESD. The downscaling model and part of the analysis used the ECMWF fifth-generation ERA5 reanalysis hourly data downloaded from Copernicus C3S. We acknowledge the data providers in the ECA&D project by Klein Tank, A.M.G. and Coauthors, 2002. Daily dataset of 20th-century surface air temperature and precipitation series for the European Climate Assessment. Int. J. of Climatol., 22, 1441-1453. Data and metadata available at https://www.ecad.eu We acknowledge the CMIP6 community for providing the climate model data, retained and globally distributed in the framework of the ESGF. The CMIP6 data and server-side computing resources for this study were made available by the German Climate Computing Centre (DKRZ) under project ID 1088.

https://doi.org/10.5194/egusphere-2024-1463
Preprint. Discussion started: 4 June 2024

References

Barnett, T. P.: Comparison of Near-Surface Air Temperature Variability in 11 Coupled Global Climate Models, Journal of Climate, 12, 511–518, https://doi.org/10.1175/1520-0442(1999)012<0511:CONSAT>2.0.CO;2, 1999.

Benestad, R.: Empirical-statistical downscaling of daily precipitation information in the Nordics, https://doi.org/10.6084/M9.FIGSHARE.25809196.V1, 2024.

Benestad, R., Sillmann, J., Thorarinsdottir, T. L., Guttorp, P., Mesquita, M. d. S., Tye, M. R., Uotila, P., Maule, C. F., Thejll, P., Drews, M., and Parding, K. M.: New vigour involving statisticians to overcome ensemble fatigue, Nature Climate Change, 7, 697–703, https://doi.org/10.1038/nclimate3393, 2017.

Benestad, R. E.: A comparison between two empirical downscaling strategies, Int. J. Climatology, 21, 1645–1668, dOI 10.1002/joc.703, 2001.

Benestad, R. E.: A new global set of downscaled temperature scenarios, Journal of Climate, 24, 2080–2098, https://doi.org/10.1175/2010JCLI3687.1, 2011.

Benestad, R. E. and Mezghani, A.: On downscaling probabilities for heavy 24-hour precipitation events at seasonal-to-decadal scales, Tellus A, 67, https://doi.org/10.3402/tellusa.v67.25954, 2015.

Benestad, R. E., Mezghani, A., and Parding, K. M.: esd V1.0, http://dx.doi.org/10.5281/zenodo.29385, 2015.

Benestad, R. E., Senan, R., and Orsolini, Y.: The use of regression for assessing a seasonal forecast model experiment, Earth System Dynamics Discussions, pp. 1–20, https://doi.org/10.5194/esd-2016-14, 2016.

Benestad, R. E., Oort, B. v., Justino, F., Stordal, F., Parding, K. M., Mezghani, A., Erlandsen, H. B., Sillmann, J., and Pereira-Flores, M. E.: Downscaling probability of long heatwaves based on seasonal mean daily maximum temperatures, Advances in Statistical Climatology, Meteorology and Oceanography, 4, 37–52, https://doi.org/https://doi.org/10.5194/ascmo-4-37-2018, 2018.

Benestad, R. E., Parding, K. M., Erlandsen, H. B., and Mezghani, A.: A simple equation to study changes in rainfall statistics, Environmental Research Letters, 14, 084 017, https://doi.org/10.1088/1748-9326/ab2bb2, 2019.

Benestad, R. E., Lutz, J., Dyrrdal, A. V., Haugen, J. E., Parding, K. M., and Dobler, A.: Testing a simple formula for calculating approximate intensity-duration-frequency curves, Environmental Research Letters, https://doi.org/10.1088/1748-9326/abd4ab, 2020.

Benestad, R. E., Mezghani, A., Lutz, J., Dobler, A., Parding, K. M., and Landgren, O. A.: Various ways of using empirical orthogonal functions for climate model evaluation, Geoscientific Model Development, 16, 2899–2913, https://doi.org/10.5194/gmd-16-2899-2023, 2023.

Benestad, R. E., Lussana, C., and Dobler, A.: A link between the global surface area receiving daily precipitation, wet-day frequency and probability of extreme rainfall, Discover Water, 4, 10, https://doi.org/10.1007/s43832-024-00063-3, 2024.

Christensen, J. H. and Christensen, O. B.: A summary of the PRUDENCE model projections of changes in European climate by the end of this century, Climatic Change, 81, 7–30, https://doi.org/10.1007/s10584-006-9210-7, 2007.

Christensen, J. H., Carter, T. R., Rummukainen, M., and Amanatidis, G.: Evaluating the performance and utility of regional climate models: the PRUDENCE project, Climatic Change, 81, 1–6, https://doi.org/10.1007/s10584-006-9211-6, 2007.

Coles, S. G.: An Introduction to Statistical Modeling of Extreme Values, Springer, London, 2001.

Deser, C., Knutti, R., Solomon, S., and Phillips, A. S.: Communication of the role of natural variability in future North American climate, Nature Climate Change, 2, 775–779, https://doi.org/doi:10.1038/nclimate1562, 2012.

https://doi.org/10.5194/egusphere-2024-1463
Preprint. Discussion started: 4 June 2024

Eyring, V., Bony, S., Meehl, G. A., Senior, C., Stevens, B., Stouffer, R. J., and Taylor, K. E.: Overview of the Coupled Model Intercomparison Project Phase 6 (CMIP6) experimental design and organisation, Geoscientific Model Development Discussions, 8, 10 539–10 583, https://doi.org/10.5194/gmdd-8-10539-2015, 2015.

Eyring, V., Bony, S., Meehl, G. A., Senior, C. A., Stevens, B., Stouffer, R. J., and Taylor, K. E.: Overview of the Coupled Model Intercomparison Project Phase 6 (CMIP6) experimental design and organization, Geoscientific Model Development, 9, 1937–1958, https://doi.org/10.5194/gmd-9-1937-2016, 2016.

Goodess, C., Osborn, T., and Hulme, M.: The identification and evaluation of suitable scenario development methods for the estimation of future probabilities of extreme weather events, Technical Report 4, Tyndall Centre, School of Environemtal Sciences, Univ. East Anglia, Norwich, 2003.

Gutowski Jr., W. J., Giorgi, F., Timbal, B., Frigon, A., Jacob, D., Kang, H.-S., Raghavan, K., Lee, B., Lennard, C., Nikulin, G., O'Rourke, E., Rixen, M., Solman, S., Stephenson, T., and Tangang, F.: WCRP COordinated Regional Downscaling EXperiment (CORDEX): a diagnostic MIP for CMIP6, Geoscientific Model Development, 9, 4087–4095, https://doi.org/10.5194/gmd-9-4087-2016, 2016.

Hawkins, E. and Sutton, R.: The potential to narrow uncertainty in regional climate predictions, Bull. Amer. Meteor. Soc., 90, p1095, 2009.

Haylock, M. R., Cawley, G. C., Harpham, C., Wilby, R. L., and Goodess, C. M.: Downscaling Heavy Precipitation Over the United Kingdom: A Comparison of Dynamical and Statistical Methods and their Future Scenarios, International Journal of Climatology, 26, 1397–1416, 2006.

Hersbach, H. and Dee, D.: ERA5 reanalysis is in production., ECMWF Newsletter 147, ECMWF, Reading, United Kingdom, www.ecmwf.int/sites/default/files/elibrary/2016/16299Â■newsletterÂ■no147Â■springÂ■2016.pdf.], 2016.

Hersbach, H., Bell, B., Berrisford, P., Hirahara, S., Horanyi, A., Munoz-Sabater, J., Nicolas, J., Peubey, C., Radu, R., Schepers, D., Simmons, A., Soci, C., Abdalla, S., Abellan, X., Balsamo, G., Bechtold, P., Biavati, G., Bidlot, J., Bonavita, M., Chiara, G., Dahlgren, P., Dee, D., Diamantakis, M., Dragani, R., Flemming, J., Forbes, R., Fuentes, M., Geer, A., Haimberger, L., Healy, S., Hogan, R. J., Holm, E., Janiskova, M., Keeley, S., Laloyaux, P., Lopez, P., Lupu, C., Radnoti, G., Rosnay, P., Rozum, I., Vamborg, F., Villaume, S., and Thepaut, J.: The ERA5 global reanalysis, Quarterly Journal of the Royal Meteorological Society, 146, 1999–2049, https://doi.org/10.1002/qj.3803, 2020.

IPCC: Climate Change 2021: The Physical Science Basis. Contribution of Working Group I to the Sixth Assessment Report of the Intergovernmental Panel on Climate Change, Tech. rep., Cambridge University Press, 2021.

Jacob, D., Teichmann, C., Sobolowski, S., Katragkou, E., Anders, I., Belda, M., Benestad, R., Boberg, F., Buonomo, E., Cardoso, R. M., Casanueva, A., Christensen, O. B., Christensen, J. H., Coppola, E., De Cruz, L., Davin, E. L., Dobler, A., Domínguez, M., Fealy, R., Fernandez, J., Gaertner, M. A., García-Díez, M., Giorgi, F., Gobiet, A., Goergen, K., Gómez-Navarro, J. J., Alemán, J. J. G., Gutiérrez, C., Gutiérrez, J. M., Güttler, I., Haensler, A., Halenka, T., Jerez, S., Jiménez-Guerrero, P., Jones, R. G., Keuler, K., Kjellström, E., Knist, S., Kotlarski, S., Maraun, D., van Meijgaard, E., Mercogliano, P., Montávez, J. P., Navarra, A., Nikulin, G., de Noblet-Ducoudré, N., Panitz, H.-J., Pfeifer, S., Piazza, M., Pichelli, E., Pietikäinen, J.-P., Prein, A. F., Preuschmann, S., Rechid, D., Rockel, B., Romera, R., Sánchez, E., Sieck, K., Soares, P. M. M., Somot, S., Srnec, L., Sørland, S. L., Termonia, P., Truhetz, H., Vautard, R., Warrach-Sagi, K., and Wulfmeyer, V.: Regional climate downscaling over Europe: perspectives from the EURO-CORDEX community, Regional Environmental Change, 20, https://doi.org/10.1007/s10113-020-01606-9, 2020.

Klein Tank, A. J. B. W., Konnen, G. P., Böhm, R., Demarée, G., Gocheva, A., Mileta, M., Pashiardis, S., Hejkrlik, L., Kern-Hansen, C., Heino, R., Bessemoulin, P., Müller-Westermeier, G., Tzanakou, M., Szalai, S., Pálsdóttir, T., Fitzgerald, D., Rubin, S., Capaldo, M., Maugeri, M.,

https://doi.org/10.5194/egusphere-2024-1463
Preprint. Discussion started: 4 June 2024

Leitass, A., Bukantis, A., Aberfeld, R., Engelen, A. F. V. v., Førland, E., Mietus, M., Coelho, F., Mares, C., Razuvaev, V., Nieplova, E., Cegnar, T., López, J. A., Dahlström, B., Moberg, A., Kirchhofer, W., Ceylan, A., Pachaliuk, O., Alexander, L. V., and Petrovic, P.: Daily dataset of 20th-century surface air temperature and precipitation series for the European Climate Assessment, International Journal of Climatology, 22, 1441–1453, 2002.

Lorenz, E. N.: Empirical Orthogonal Functions and Statistical Weather Prediction, Sci. rep. 1, Department of Meteorology, MIT, USA, Cambridge, Massachusetts, https://eapsweb.mit.edu/sites/default/files/Empirical_Orthogonal_Functions_1956.pdf, 1956.

Lussana, C., Benestad, R., and Dobler, A.: Changes in regional daily precipitation intensity and spatial structure from global reanalyses, International Journal of Climatology, 44, 1135–1153, https://doi.org/10.1002/joc.8375, 2024.

Maraun, D., Widmann, M., Gutiérrez, J. M., Kotlarski, S., Chandler, R. E., Hertig, E., Wibig, J., Huth, R., and Wilcke, R. A.: VALUE: A framework to validate downscaling approaches for climate change studies, Earth's Future, 3, 2014EF000 259, https://doi.org/10.1002/2014EF000259, 2015.

Mezghani, A., Dobler, A., Haugen, J. E., Benestad, R. E., Parding, K. M., Piniewski, M., Kardel, I., and Kundzewicz, Z. W.: CHASE-PL Climate Projection dataset over Poland – bias adjustment of EURO-CORDEX simulations, Earth System Science Data, 9, 905–925, https://doi.org/https://doi.org/10.5194/essd-9-905-2017, 2017.

Mezghani, A., Dobler, A., Benestad, R., Haugen, J. E., Parding, K. M., Piniewski, M., and Kundzewicz, Z. W.: Sub-sampling impact on the climate change signal over Poland based on simulations from statistical and dynamical downscaling, Journal of Applied Meteorology and Climatology, https://doi.org/10.1175/JAMC-D-18-0179.1, 2019.

Nychka, D.: LatticeKrig: A multi-resolution spatial model for large data., in: Spatial Statistics for Environmental and Energy Challenges - Workshop 2014, Thuwal, Saudi Arabia, 2014.

Oguz, E. A., Benestad, R. E., Parding, K. M., Depina, I., and Thakur, V.: Quantification of climate change impact on rainfall-induced shallow landslide susceptibility: a case study in central Norway, Georisk: Assessment and Management of Risk for Engineered Systems and Geohazards, pp. 1–24, https://doi.org/10.1080/17499518.2023.2283848, 2024.

Parding, K. M., Benestad, R., Mezghani, A., and Erlandsen, H. B.: Statistical Projection of the North Atlantic Storm Tracks, Journal of Applied Meteorology and Climatology, 58, 1509–1522, https://doi.org/10.1175/JAMC-D-17-0348.1, 2019.

Pryor, S., School, J. T., and Barthelmie, R. J.: Empirical downscaling of wind speed probability distributions, Journal of Geophysical Research, 110, D19 109, https://doi.org/doi:10.1029/2005JD005899, 2005.

Pryor, S., School, J. T., and Barthelmie, R. J.: Winds of change? Projections of near-surface winds under climate change scenarios, Geophys. Res. Lett., 33, 2006.

Rampal, N., Hobeichi, S., Gibson, P. B., Baño-Medina, J., Abramowitz, G., Beucler, T., González-Abad, J., Chapman, W., Harder, P., and Gutiérrez, J. M.: Enhancing Regional Climate Downscaling through Advances in Machine Learning, Artificial Intelligence for the Earth Systems, 3, 230 066, https://doi.org/10.1175/AIES-D-23-0066.1, 2024.

Schulzweida, U.: CDO User Guide: Climate Data Operator, Version 2.0.0, October 2021, Tech. rep., MPI for Meteorology, https://code.mpimet.mpg.de/projects/cdo/embedded/cdo.pdf, 2021.

Takayabu, I., Kanamaru, H., Dairaku, K., Benestad, R., Storch, H. v., and Christensen, J. H.: Reconsidering the quality and utility of downscaling, Journal of the Meteorological Society of Japan, 94A, 31–45, https://doi.org/10.2151/jmsj.2015-042, 2015.

Trenberth, K. E., Dai, A., Rasmussen, R. M., and Parsons, D. B.: The Changing Character of Precipitation, Bulletin of the American Meteorological Society, 84, 1205–1218, https://doi.org/10.1175/BAMS-84-9-1205, 2003.

https://doi.org/10.5194/egusphere-2024-1463
Preprint. Discussion started: 4 June 2024

535 Wilks, D. S.: Statistical methods in the atmospheric sciences, no. v. 91 in International geophysics series, Academic Press, Amsterdam ; Boston, 2nd ed edn., 2006.

https://doi.org/10.5194/egusphere-2024-1463
Preprint. Discussion started: 4 June 2024

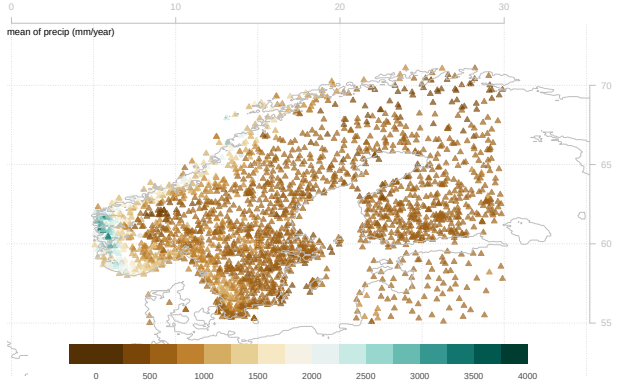

Figure 1. Map showing the rain gauge station network from ECA&D used as predictands in the empirical-statistical downscaling of 24-hr precipitation statistics. The colour legend shows the mean annual total precipitation.

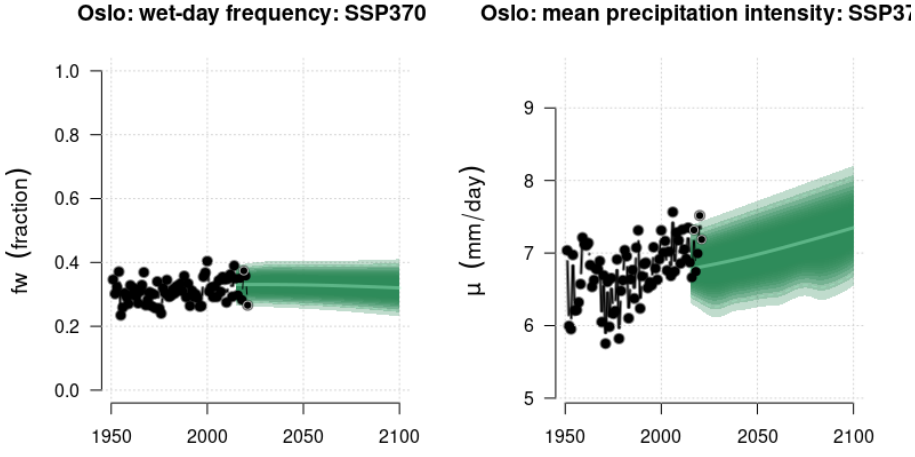

Figure 2. Ensembles of downscaled wet-day frequency f_w and wet-day mean precipitation μ for Oslo based on the SSP370 emission scenario. Black symbols show annual such aggregated statistics estimated from rain gauge measurements from Oslo-Blindern and the green shading mark the ensemble spread of corresponding downscaled results.

https://doi.org/10.5194/egusphere-2024-1463
Preprint. Discussion started: 4 June 2024

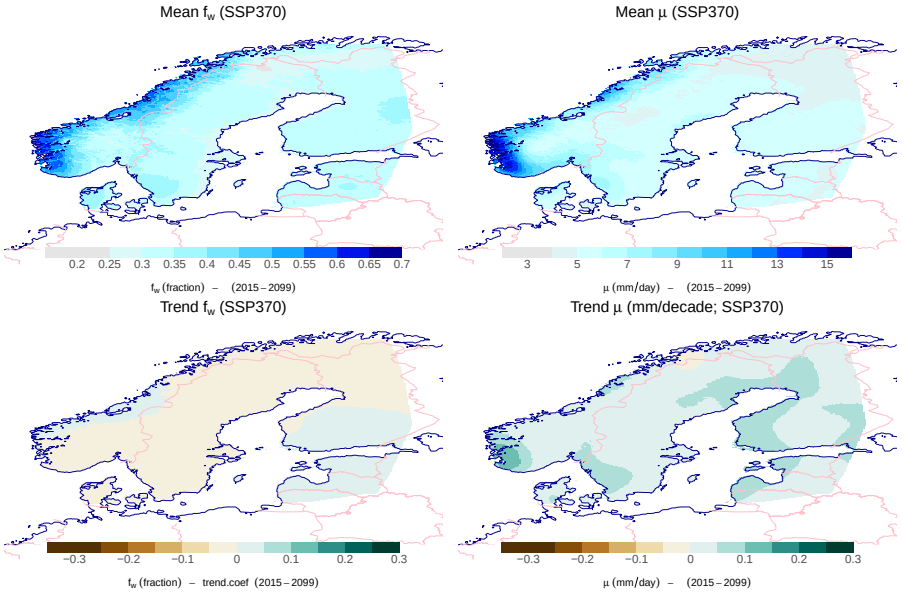

Figure 3. Maps of downscaled mean f_w (upper left) and μ (upper right) as well as trend estimates (lower).

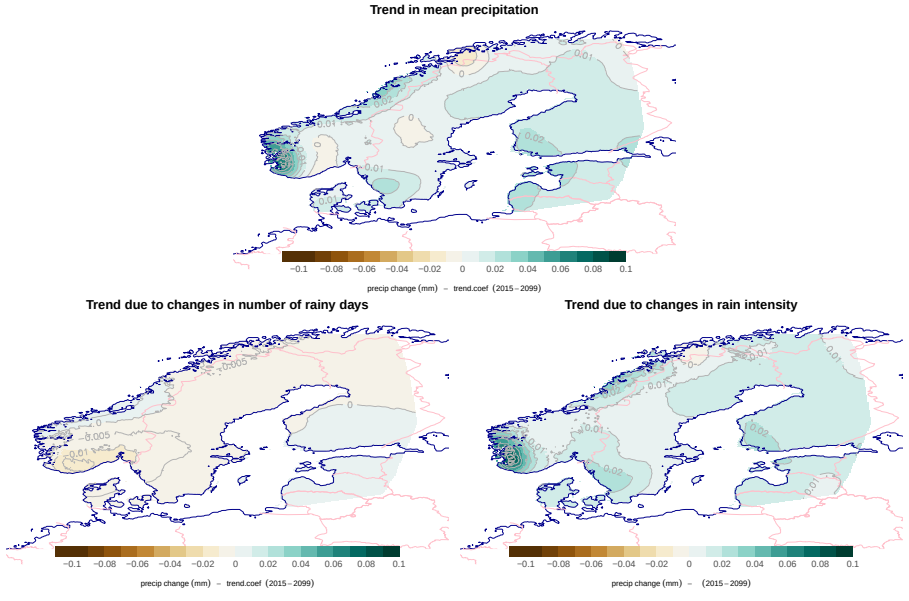

Figure 4. Estimated trend in mean precipitation $\overline{x} = f_w \mu$ and the contribution due to wet-days f_w and mean intensity μ.

https://doi.org/10.5194/egusphere-2024-1463
Preprint. Discussion started: 4 June 2024

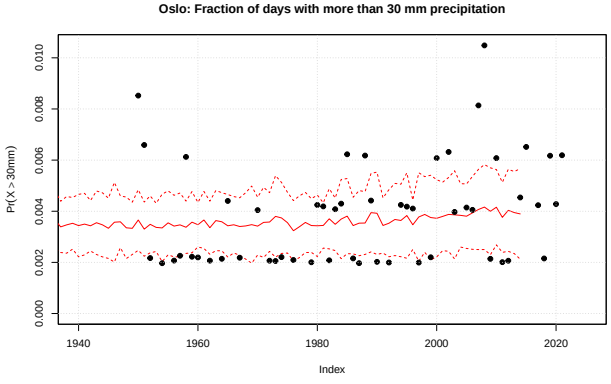

Figure 5. Observed and estimated fraction of days per year in Oslo with more than 30 mm. Solid line shows the ensemble mean and dashed lines the ensemble mean plus or minus the ensemble standard deviation.

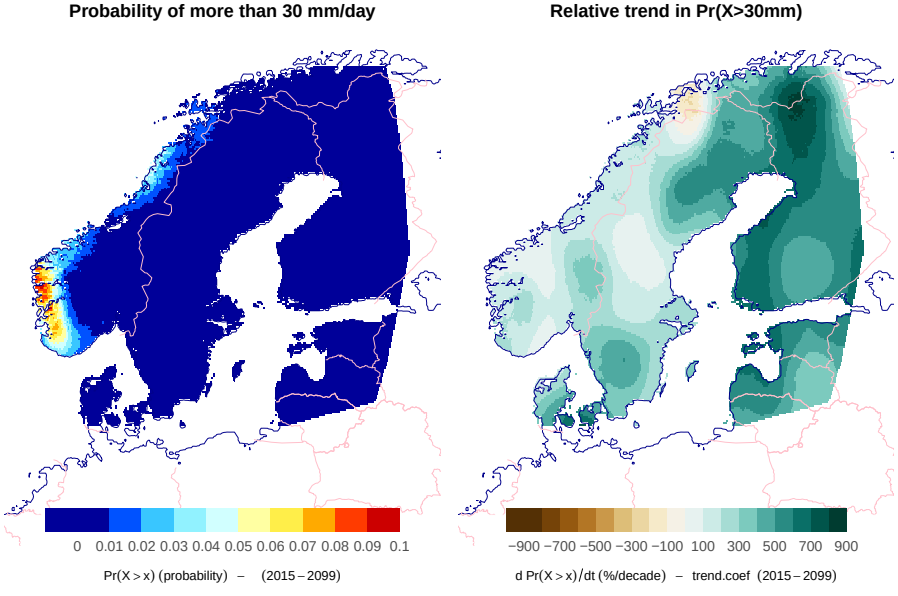

Figure 6. Estimates of the mean probability of more than 30 mm precipitation in 24 hours according to $Pr(X > x) = f_w \exp(-x/\mu)$ and based on downscaled f_w (right) and μ (left), estimates of the future trend (middle), and proportional trend (right). These results are based on the SSP370 emission scenario.

https://doi.org/10.5194/egusphere-2024-1463
Preprint. Discussion started: 4 June 2024

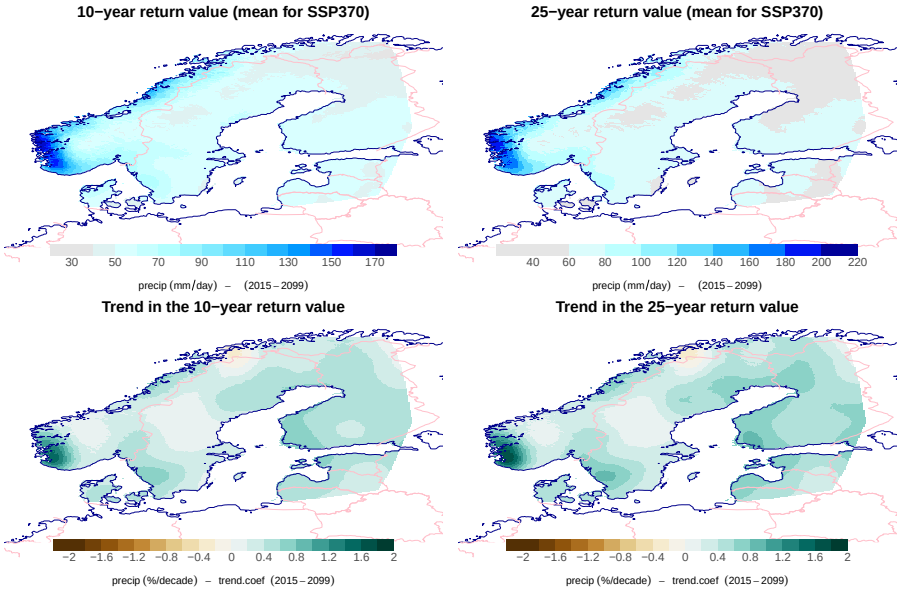

Figure 7. Estimates of the 10-year and 25-year return-values based on the expression $x_\tau = \alpha\mu \ln(f_w \tau)$ (Benestad et al., 2019), and their future trend estimates (lower). The results are based on the SSP370 emission scenario and the CMIP6 ensemble mean downscaled f_w (right) and μ.

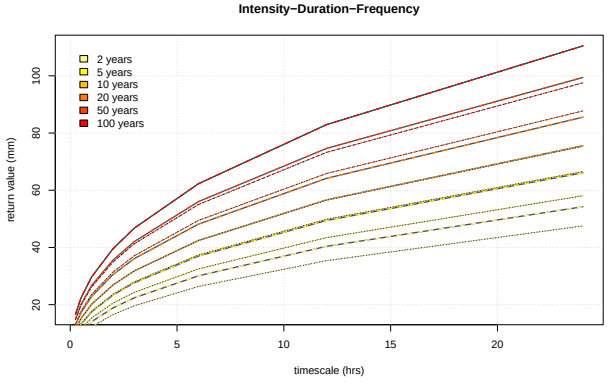

Figure 8. Estimate of intensity-duration-frequency curves for Oslo-Blindern based on downscaled f_w and μ (thick solid-dashed) and their future trend estimates (thin dotted). These results are based on the SSP370 emission scenario and the expression $x_\tau(L) = \alpha\mu(L/24)^\zeta \ln(f_w \tau)$ (Benestad et al., 2020).

https://doi.org/10.5194/egusphere-2024-1463
Preprint. Discussion started: 4 June 2024

Table 1. The ensemble mean and standard deviation of the wet-day frequency f_w and wet-day mean precipitation μ projected for 2071–2100 for a selection of locations.

Location	emission scenario	$\overline{f_w} \pm \sigma_f$	$\overline{\mu} \pm \sigma_\mu$
Geiranger	SSP370	0.44 ± 0.06	9.24 ± 0.78
	SSP126	0.44 ± 0.06	9.1 ± 0.78
	SSP245	0.44 ± 0.06	9.12 ± 0.8
	SSP585	0.44 ± 0.05	9.28 ± 0.9
Halden	SSP370	0.34 ± 0.05	7.18 ± 0.43
	SSP126	0.34 ± 0.05	7.06 ± 0.35
	SSP245	0.34 ± 0.05	7.16 ± 0.46
	SSP585	0.33 ± 0.05	7.24 ± 0.44
Helsinki	SSP370	0.32 ± 0.04	5.89 ± 0.34
	SSP126	0.32 ± 0.04	5.62 ± 0.28
	SSP245	0.32 ± 0.04	5.75 ± 0.36
	SSP585	0.31 ± 0.04	6.05 ± 0.43
Malmö	SSP370	0.3 ± 0.02	5.72 ± 0.25
	SSP126	0.31 ± 0.02	5.47 ± 0.22
	SSP245	0.3 ± 0.03	5.6 ± 0.29
	SSP585	0.3 ± 0.03	5.86 ±0.34
Oslo	SSP370	0.32 ± 0.04	7.24 ± 0.41
	SSP126	0.32 ± 0.04	6.99 ± 0.35
	SSP245	0.32 ± 0.04	7.15 ± 0.45
	SSP585	0.32 ± 0.04	7.38 ± 0.47
Stockholm	SSP370	0.28 ± 0.03	5.31 ± 0.21
	SSP126	0.29 ± 0.03	5.15 ± 0.17
	SSP245	0.29 ± 0.03	5.24 ± 0.22
	SSP585	0.28 ± 0.03	5.39 ± 0.27
Tallinn	SSP370	0.34 ± 0.04	5.67 ± 0.31
	SSP126	0.35 ± 0.04	5.39 ± 0.28
	SSP245	0.34 ± 0.04	5.52 ± 0.36
	SSP585	0.33 ± 0.04	5.82 ± 0.4
Vestervig	SSP370	0.37 ± 0.04	6 ± 0.18
	SSP126	0.37 ± 0.04	6.01 ± 0.16
	SSP245	0.37 ± 0.04	6.01 ± 0.18
	SSP585	0.36 ± 0.05	5.99 ± 0.2